A&A manuscript no.
(will be inserted by hand later)

Your thesaurus codes are:
11 (11.09.1; 11.09.5; 11.19.2; 13.09.1)

ASTRONOMY
AND
ASTROPHYSICS
26.9.1996

ISOPHOT Maps of NGC 6946 in the range λ 60 - 200 $\mu m^\star$

R. J. Tuffs[1], D. Lemke[2], C. Xu[1], J. I. Davies[3], C. Gabriel[4,⋆⋆], I. Heinrichsen[1,4], G. Helou[5], H. Hippelein[2], N. Y. Lu[5], and D. Skaley[1,6]

[1] Max–Planck–Institut für Kernphysik, Saupfercheckweg 1, D-69117 Heidelberg, Federal Republic of Germany
[2] Max–Planck–Institut für Astronomie, Königstuhl 17, D-69117 Heidelberg, Federal Republic of Germany
[3] Department of Physics and Astronomy, University of Wales College of Cardiff, United Kingdom
[4] European Space Agency Satellite Tracking Station, Apartado 50727 - 28080 Madrid, Spain
[5] IPAC 100-22, California Institute of Technology, Pasadena, CA 91125, United States of America
[6] Max–Planck–Institut für Radioastronomie, Auf dem Hugel 69, D-53121 Bonn, Federal Republic of Germany

Received ??; accepted ??

Abstract. We present maps of NGC 6946 at λ 61 and 205 μm as well as scans through the galaxy at these and at 8 intermediate wavelengths. The bulk of the FIR luminosity arises from a diffuse disk component which extends beyond the 25 mag arcsec^{-2} B isophote to at least the radius corresponding to the sensitivity limit. A FIR emission counterpart to the outlying HI disk is seen at both 61 and 205 μm, for which a dust to HI mass ratio of 0.0046 is inferred from the 205 μm brightness assuming a dust temperature of 15 K. The disk scale length at both λ 61 and 205 μm is similar to that seen in R-band.

Key words: galaxies – star formation – dust

1. Introduction

IRAS observations of nearby spiral galaxies have shown that the size of the FIR disk is comparable with that of the optical disk, both in terms of e-folding scale length (Walterbos & Schwering 1987; Rice et al. 1990), and in terms of size measured down to the sensitivity level (Rice et al. 1988). The broad spectral energy distribution of continuum emission in the λ 12 - 100 μm range is generally interpreted in terms of dust models (eg Draine & Anderson 1985, Désert et al. 1990) incorporating large molecules and very small grains (VSG) transiently heated to relatively high temperatures by individual UV photons in the interstellar radiation field (ISRF). Such models can also account for the relatively constant 60/100 μm colour profiles of disks of nearby galaxies by attributing a substantial fraction of the 60 μm emission to VSGs, as found for M31 by Walterbos & Schwering (1987).

ISO permits deeper, diffraction-limited, and spectrally better-sampled studies of the morphology of galaxian disks. It is particularly sensitive to the detection of cold large grains in thermal equilibrium with the Interstellar Radiation Field, expected to dominate the spectral region beyond 100 μm not covered by IRAS. Here we present maps of NGC 6946 at λ 61 and 205 μm as well as scans through the galaxy at these and at 8 intermediate wavelengths. A companion paper by Lu et al. (1996) compares the λ61 μm map with radio data.

2. Observations and Data Reduction

The observations were made on 9th January 1996 as part of a program to verify and commission the diffraction-limited photometric mapping mode of the ISOPHOT instrument (Lemke et al. 1996) in the λ 60 - 200 μm range. NGC 6946 was mapped at the shortest and longest available wavelengths (61 and 205 μm) using the C100 3x3 and the C200 2x2 detector arrays, respectively. A field extending about twice the 11$'$.5 visual major axis of the galaxy was covered in the in-scan direction (ie parallel to the chopper motion) at both wavelengths, sampled at 15$''$ x 23$''$and 31$''$ x 46$''$with the C100 and C200 detectors, respectively. In addition, scans of length 14$'$.6 (C100 detector) and 20$'$.1 (C200 detector) were performed in the passbands given in Table 1. All maps and scans were centred on the 1950 position of the nucleus at $\alpha\, 20^h 33^m 48^s.8$ $\delta\, 59^o 58' 50''$ and performed sequentially at a scan P.A. of 107^o E from N.

Send offprint requests to: R. J. Tuffs

⋆ Based on observations with ISO, an ESA project with instruments funded by ESA Member States (especially the PI countries: France, Germany, the Netherlands and the United Kingdom) and with the participation of ISAS and NASA

⋆⋆ affiliated to the Astrophysics Division, Space Science Department, European Space Agency

The data was reduced using the ISOPHOT Interactive Analysis Package (Gabriel et al 1996) for editing, deglitching, non-linearity corrections and flat-fielding. The geometrical overlap between map and detector pixels was used to grid the data onto regularly sampled maps in instrumental coordinates using the spacecraft attitude data. The theoretical FWHM of the point-spread functions in the in-scan direction on the maps produced in this way is given in Table 1. Calibration was not possible using the internal Fine Calibration Sources due to a cosmic hit on the RAM of the on-board computer. A relative calibration between different filters, accurate to 40%, was derived from observations of standard calibration sources. Because detector responsivities can vary by a factor of two during an orbit, the absolute calibrations for the C100 and the C200 detectors were fixed by comparing the ISO maps of NGC 6946 at 61 and 205 μm with IRAS and KAO maps made in similar wavebands by Engargiola (1991). Thus, all data taken with the C100 detector was multiplied by the factor of 0.58 required to scale the spatially integrated flux density within a radius of 5$'\!.$6 from the nucleus in the 61 μm ISO map to the 147 ± 29 Jy measured by Engargiola (1991) from the same region of a 60 μm IRAS map. The corresponding correction factor for the C200 detector was 0.54, obtained by comparing the integrated flux density measured by ISO at 205 μm within a radius of 2$'\!.$5 from the nucleus with the value of 226 ± 50 Jy obtained by Engargiola (1991) from a KAO map of the inner disk at 200 μm.

Table 1. Wavelengths and Bandpasses in micron and Angular Resolutions in arcsec for the Filters used

λ_c	61	67	80	95	103	119	161	174	185	205
$\Delta\lambda$	24	58	49	51	44	47	82	89	72	67
$\Delta\theta$	52	53	55	57	58	104	110	112	115	117

2.1. *Image quality*

The brightness of the nucleus is thought to have been underestimated relative to the disk in the 61 – 103 μm measurements because the time scale of the C100 detector to react to the illumination step is only comparable to the interval between chopper pointings. A similar transient behaviour in detector responsivity may potentially tend to smooth out gradients in the disk, though the similarity of the ISOPHOT 61μm map to the IRAS CPC 50μm map by van Driel et al (1995) suggests this effect is not serious, at least in the inner disk.

Stray light in the telescope beam, originating from the bright central regions of the galaxy, may potentially mimic a faint extended disk. However, initial investigations suggest this effect cannot account for the brightness of the extended disk emission (see radial beam profile given in Lemke et al. 1996). A quantitative treatment of the stray light and detector transient artifacts for the NGC6946 data will be given in a future paper.

3. Morphology of NGC 6946 in the FIR

The ISOPHOT data provide deeper and more precise measurements of the extended low-surface brightness structure of the disk of NGC 6946 than previously possible. The 61 μm map of NGC 6946 (Figure 1a) shows faint FIR emission extending almost as far as the extinction corrected 25 mag arcsec^{-2} B-band isophote, quoted by de Vaucouleurs et al (1991) as having a diameter D(25) = 16$'\!.$6. It may be considered as the FIR counterpart of the faint optical disk as seen in the R-band image of NGC 6946 of Figure 1b and the extended HI emission (Boulanger & Viallefond 1992) in the outer disk. The comparison between the 61 μm and R-band images shows that although spiral arms can be discerned in the FIR, the bulk of the 61 μm emission appears to originate from a diffuse disk component. This disk component appears to be elongated along a p.a. of $\sim 100^o$ in both the 61 μm and R-band images, rather than the 69^o of the inner disk.

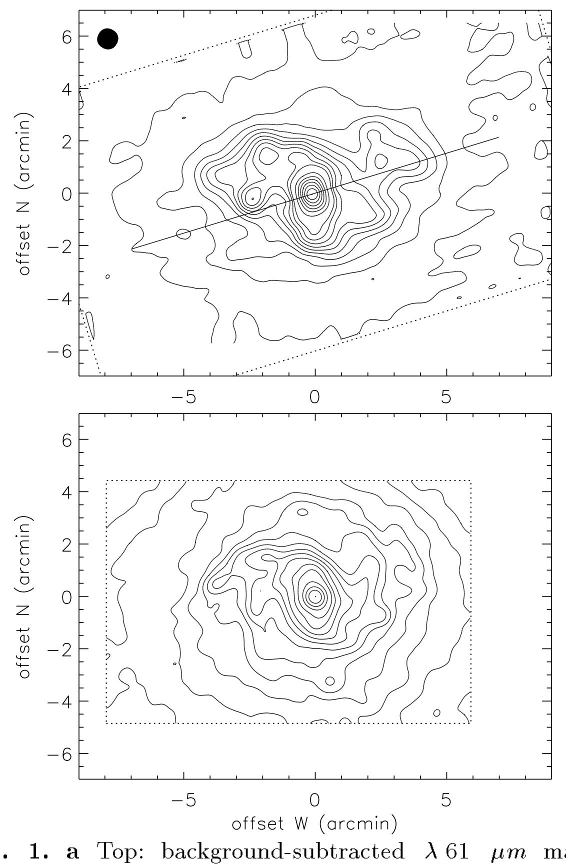

Fig. 1. a Top: background-subtracted λ 61 μm map of NGC 6946. Dotted lines mark the boundary of the area mapped, and the path of the linear scans through the nucleus with the C100 detector is shown. Contours levels (MJy sterad^{-1}) are 3.4, 6.8 to 68 in steps of 6.8, and 111 to 226 in steps of 19. **b** R-band image of NGC 6946, taken with the 70 cm telescope at the MPI für Astronomy in Heidelberg with a 790×1155 pixel CCD, and smoothed to the same beam as the ISOPHOT 61 μm map. The contour scaling is linear.

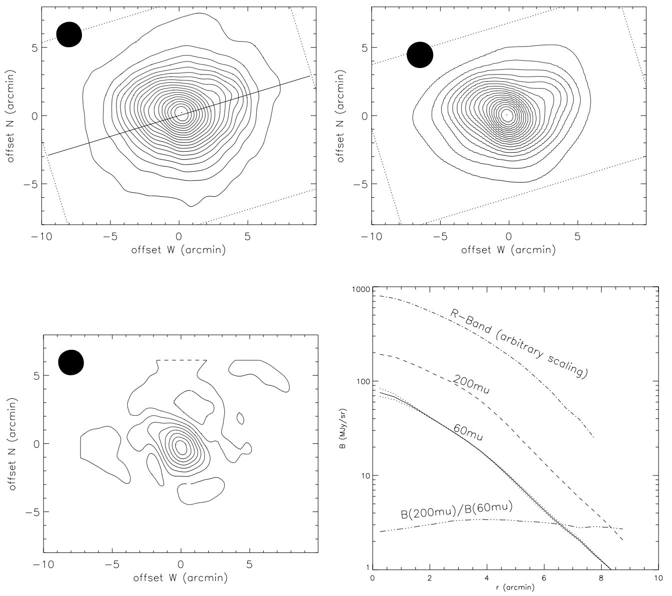

Fig. 2. **a** Upper left: background-subtracted λ 205 μm map of NGC 6946. Dotted lines mark the boundary of the area mapped, and the path of the linear scans through the nucleus with the C200 detector is shown. Contours levels (MJy sterad^{-1}) range from 10.8 to 217 in steps of 10.8. **b** Upper right: background-subtracted λ 61 μm map of NGC 6946, smoothed to the same beam as the 205 μm map. Contours levels (MJy sterad^{-1}) range from 4.3 to 86 in steps of 4.3. **c** Lower left: 61 μm map multiplied by 3.76 minus 205 μm map. Contours levels (MJy sterad^{-1}) range from -9.3 to 52 in steps of 6.2. **d** Lower right: radial profiles at 61 & 205 μm and in R-band after baseline subtraction and smoothing to a common resolution. The dotted lines indicate the effect of changing the resolution of the smoothed 61 μm map by $\pm$ 10%.

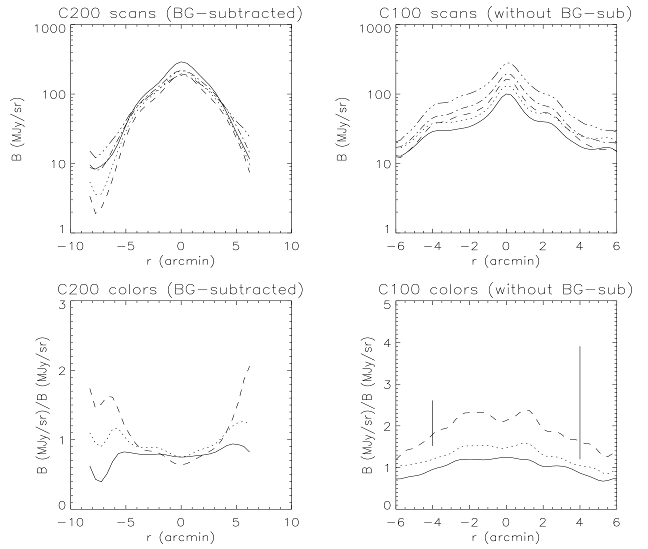

Fig. 3. **a** Background-subtracted scan profiles made with the C200 detector at 119 μm (full line), 162 μm (dotted), 174 μm (dashed), 185 μm (dot-dash) and 205 μm (dash triple dot). **b** Ratios 161/119μm (line) 185/119μm (dotted) and 205/119μm (dashed) for scans made with the C200 detector. **c** Scan profiles (without background-subtraction) made with the C100 detector at 67 μm (full line), 61 μm (dotted), 80 μm (dashed), 95 μm (dot-dash) and 103 μm (dash triple dot), convolved to a common resolution of 80″FWHM. **d** Ratios 80/61μm (line) 95/61μm (dotted) and 103/61μm (dashed) for scans made with the C100 detector (without background-subtraction). The trend towards warmer colours at the ends of the scans is due to the larger fraction of background zodiacal emission there.

There is a strong similarity between the morphology of the 205 μm map and the 61 μm map smoothed to a common resolution (Figure 2a,b). Indeed, it is possible to accurately remove the diffuse disk emission from the 61 μm map by subtracting a scaled 205 μm map, leaving a residue (Figure 2c) of warm emission from the nucleus and the bar. Thus at these wavelengths the morphology of NCG 6946 is well approximated by a superposition of warmer emission from the nucleus and a relatively uniformly coloured colder diffuse disk component. The radial profiles shown in Figure 2d follow an exponential law at least as far as 8′($\sim$ 23kpc assuming a distance of 10 Mpc to NGC 6946). The disk scale length at both 61 and 205 μm is similar to that seen in the R-band, with a colour ratio changing by less than 40%, a result that is insensitive to the precise beam size assumed for the 205 μm map. This is flatter than the variation of the colour ratio in the cross-scan direction which is about a factor of 2, possibly due to transient behaviour of the C100 detector.

The scans, depicted in Figure 3 as brightness and colour profiles at selected wavelengths, indicate that most of the increase in the 205:61 μm ratio occurs over the 119-205 μm range covered by the C200 detector. In this range emission from NGC 6946 dominates the background over the 12′ strip depicted, so the background could be subtracted and the variation of colour with position may be taken as intrinsic to NGC 6946. A trend towards colder emission in the outer disk region, is seen throughout the 119-205μm range, as expected for large-grain emission.

By contrast, the scans in the C100 detector were too short for an accurate background subtraction (Fig. 3c,d). The large change in colour between positions towards the inner and outer disk seen on the C100 detector scans therefore reflects the transition from NGC 6946-dominated emission to background emission, which is much warmer due to the zodiacal contribution. This effect dominates large-scale colour gradients intrinsic to the unexpectedly extended emission in the C100 range. However the relative constancy of the 205/61μm colour ratio derived from the maps (which measured the background adequately), coupled with the evidence from the C200 detector scans for decreasing colour temperatures in the disk, indirectly implies relatively constant colour temperatures with radial position in the C100 detector range. Taking into account the presence of the warm nuclear and bar emission, seen as a dip in the 103/61 and 95/61μm brightness ratios in Figure 3d, the ISOPHOT colour profiles do not deviate significantly from the 50/100μm colour profile measured from a 12′ x 9′ IRAS CPC map by van Driel et al. (1995).

The small-scale structure seen on the C100 detector scans and the 61μm maps corresponds well to the H_α map at similar resolution by Engargiola (1991). As found for HII region complexes in M101 and M51 by Hippelein et al (1996), the colour profiles measured by C100 detector (Fig.3d) indicate warmer emission from the HII region complexes than the disk. We note however that even at 61μm, the small scale structures in the map and scans cause perturbations of only $< 40\%$ of the underlying smooth disk emission. Even though this is in part due to the relatively large beam, it supports the conclusion that the diffuse emission is the dominant component.

4. Discussion

Our results for NGC 6946 are in accordance with the general IRAS result that the disk scale-length of late-type galaxies in the FIR is comparable to that in the optical. However, the deeper ISOPHOT maps show emission out to r=$8'$ from the nucleus of NGC 6946, almost as far as the extinction-corrected D(25) isophote. Boulanger & Viallefond (1992) reported detection of HI gas out to r$\sim 15'$ for this galaxy, so the extended FIR emission detected by ISO may be due to dust associated with this gas. This dust is less likely to be heated by ionising radiation from very massive stars, given that little H_α emission has been seen beyond r$\sim 6'$ (Engargiola 1991; Devereux and Young 1993). The dust could be heated by the optical radiation which, as shown by the *R*-band radial profile, has a similar scale length to the FIR radiation. It might also be heated by the non-ionizing UV radiation from intermediate massive stars. which often has a larger scale length than the optical radiation (Rice et al. 1990). Unfortunately, although NGC 6946 has been detected at 2000 A (Donas et al. 1987) no UV map of the galaxy is available.

The constancy of the 61/205μm brightness ratio (Fig.2) in the diffuse disk to within 40% while the radiation intensity changes by about a factor of 20 suggests that the FIR colour ratio is very insensitive to the intensity of the interstellar radiation field. A similar result was obtained by Hippelein et al. (1996) for M101 and M51. Given the uncertainties discussed in Section 2.1, it is difficult to explain this result using the current grain models, even those incorporating VSGs, if smoothly distributed ISRF is assumed. For example, according to the grain model of Désert et al. (1990) the colour gradient of a factor of 2 seen in the cross-scan direction would require the IRSF to vary only between 4 and 1 times the solar ISRF between the nucleus and the outer disk, even if the abundance of VSG is a factor of 2 higher in NGC 6946 than in the solar neighbourhood. On the other hand, the constancy of the FIR colours may be due to the fluctuations of the ISRF within the beam (the $\sim 2'$ beam for the 205μm map corresponds to an area of size of about 6 kpc in the NGC 6946 disk) in which case the FIR emission, in particular in the outer region of the disk, may be dominated by some relatively bright spots where the FIR colours correspond to the intensity of local ISRF rather than to its large scale average. ISO observations of Galactic cirrus (e.g. Laureijs et al. 1996) will certainly help to answer this question.

Although the lack of strong colour gradients in the C100 detector range may indicate an overabundance in VSG in NGC 6946, the 205μm emission should still be dominated by large grains in thermal equilibrium with the ISRF, as shown by the radial decrease in colour temperature in the C200 detector range. This enables an estimate of the dust-to-gas mass ratio in the outermost regions of the disk to be made by comparing the radial profile in the 205μm emission (Figure 3d) with that of the HI brightness from Figure 10 of Boulanger & Viallefond (1992). Using the model of Draine & Lee (1984) for large Silicate grains, the column density of 15 K dust corresponding to the 2 MJy sterad^{-1} seen at $8\farcm8$ from the nucleus (25.6 kpc for an assumed distance of 10 Mpc) is 1.3 10^5 $M_\odot$ kpc^{-2}, assuming a ν^2 grain emissivity law. The corresponding HI column density is 3.6 10^7 $M_\odot$ kpc^{-2}, implying a dust-to-gas ratio of 0.0046 by mass. This result is somewhat temperature sensitive; the dust-to-gas ratio varies between 0.0028 and 0.013 for grain temperatures varying between 20 and 10 K respectively. It is nevertheless comparable with the dust to HI mass ratio $\sim$0.004 derived from the extinction of background galaxies 23.2 kpc from the nucleus of M31 (Cuillandre et al. 1996).

Acknowledgements. We would like to thank everyone associated with the ISO mission for their dedication to this enterprise over the last 13 years. We particularly thank the ISOPHOT instrument dedicated team for their heroic support during the performance verification phase, and Heinz Völk for discussions, and an anonymous referee for helpful comments.

References

Boulanger, F., & Viallefond, F. 1992, A&A 266, 37
Cuillandre, J.-C. et al. 1996, A&A in press
Désert, F.-X., Boulanger, F., Puget, J.L. 1990, A&A 237, 215
de Vaucouleurs, G. et al., 1991, Third Reference Catalog of Bright Galaxies (Springer)
Devereux, N.A., & Young, J.S. 1993, AJ 106, 948
Donas, J., et al., 1987, A&A 180, 12
Draine, B.T. & Lee, H.M. 1984 ApJ 285, 89
Draine, B.T. & Anderson, N., 1985, ApJ 292, 494
Engargiola, G., 1991, ApJ Supp. 76, 875
Gabriel, C., et al., 1996, the PIA Users Manual, available from ESA/ISO Ground Observatory VILSPA or MPI Astronomie Heidelberg.
Hippelein, H. et al. 1996, (this volume)
Laureijs, R. et al. 1996, (this volume)
Lemke, D. et al. 1996, (this volume)
Lu, N.Y. et al. 1996, (this volume)
Rice, W. et al. 1988, A&ASS 68, 91
Rice, W., et al., 1990, ApJ 358, 428
van Driel, W., et al., 1995, A&A 298, L41
Walterbos, R.A.M. & Schwering, 1987, A&A 237, 180, 27

This article was processed by the author using Springer-Verlag
LaTeX A&A style file *L-AA* version 3.